

AN EXTENDED X-RAY OBJECT EJECTED FROM THE PSR B1259–63/LS 2883 BINARY

GEORGE G. PAVLOV¹, JEREMY HARE², OLEG KARGALTSEV², BLAGOY RANGELOV², MARTIN DURANT³

Draft version October 9, 2018

ABSTRACT

We present the analysis of the *Chandra X-ray Observatory* observations of the eccentric γ -ray binary PSR B1259–63/LS 2883. The analysis shows that the extended X-ray feature seen in previous observations is still moving away from the binary with an average projected velocity of $\approx 0.07c$ and shows a hint of acceleration. The spectrum of the feature appears to be hard (photon index $\Gamma \approx 0.8$) with no sign of softening compared to previously measured values. We interpret it as a clump of plasma ejected from the binary through the interaction of the pulsar with the decretion disk of the O-star around periastron passage. We suggest that the clump is moving in the unshocked relativistic pulsar wind (PW), which can accelerate the clump. Its X-ray emission can be interpreted as synchrotron radiation of the PW shocked by the collision with the clump.

Subject headings: pulsars: individual (B1259–63) — X-rays: binaries — stars: neutron — stars: early-type — stars: individual (LS 2883)

1. INTRODUCTION

High-mass γ -ray binaries (HMGBs) consist of a compact object (i.e., a black hole or a neutron star) and a massive (early-B or late-O type) star. Only one of the few known HMGBs, B1259–63/LS 2883 (hereafter B1259), has a compact object that has been detected as a radio pulsar. The pulsar has the following properties: period $P=47.8$ ms, characteristic age $\tau = P/2\dot{P} = 330$ kyr, spin-down power $\dot{E}=8.3\times 10^{35}$ erg s⁻¹, magnetic field $B = 3.3 \times 10^{11}$ G, and distance $d \approx 2.3$ kpc (Johnston et al. 1992). The pulsar’s companion is a fast-rotating O star, with mass $M_* \approx 30M_\odot$ and luminosity $L_* = 6.3 \times 10^4 L_\odot$ (Negueruela et al. 2011), and an equatorial decretion disk⁴, which is inclined at an angle of $\approx 35^\circ$ to the orbital plane (Melatos et al. 1995; Shannon et al. 2014). The system has an orbital period $P_{\text{orb}} = 1236.7$ days, an eccentricity $e = 0.87$, a semi-major axis $a \approx 7\text{AU}$, and an inclination angle $i \approx 23^\circ$ (Negueruela et al. 2011). The pulsar is eclipsed for about one month around periastron (Johnston et al. 2005) when it is moving through the decretion disk and dense wind of its companion star. During the pulsar eclipse, peaks of nonpulsed radio emission were observed, centered at ≈ 5 days before periastron and ≈ 20 days after periastron, with the relative strengths of the peaks varying from cycle to cycle. Ball et al. (1999) interpreted it as synchrotron radiation of electrons accelerated during the pulsar passages through the decretion disk.

B1259 has been extensively studied in X-rays and γ -rays. The X-ray emission from B1259 showed no pulsa-

tions. It was interpreted as synchrotron radiation from relativistic pulsar wind (PW) leptons accelerated at the shock between the PW and the massive star outflow (Tavani & Arons 1997). Multi-epoch measurements with numerous X-ray observatories revealed binary phase dependences of the flux, photon index, and absorption column density (Chernyakova et al. 2006, 2009). Within the same orbital cycle, the strongest variations are seen around periastron. In particular, the X-ray light curve shows two peaks corresponding to first and second passages of the pulsar through the disk ($\approx 20-4$ days before periastron and $\approx 10-50$ days after periastron), while the hydrogen column density, $N_H \approx 3 \times 10^{21}$ cm⁻² during most of the cycle, increases by a factor of 2 during and between the two disk passages, confirming the presence of additional absorbing matter at these binary phases.

This unique system is one of the few HMGBs whose flaring in the GeV energy range was seen by the *Fermi* Large Area Telescope. The GeV flares of B1259 were detected soon after the pulsar passed through periastron in 2010 and 2014, while no GeV emission was seen when it was far from periastron (Abdo et al. 2011; Tam et al. 2011, 2015). The flares started $\approx 20-25$ days after the epochs of periastron and lasted roughly 1–2 months. This GeV emission could be synchrotron radiation from PW electrons accelerated to energies ~ 100 TeV in the intra-binary shock, or inverse Compton (IC) scattering of photons emitted by the massive companion off electrons with energies $\sim 1-10$ GeV (Abdo et al. 2011).

In the TeV energy range, B1259 has been observed by the H.E.S.S. observatory (Aharonian et al. 2005, 2009). Variable TeV emission was detected around the periastron passages of 2004 and 2007, with light curves similar to those of the nonpulsed radio emission. No signatures of TeV emission enhancement were detected at the times of GeV flares after the 2010 and 2014 periastron passages (Abdo et al. 2011; Malyshev et al. 2014). Several models have been developed to explain the TeV emission, such as IC scattering of stellar photons off ultra-relativistic electrons (Aharonian et al. 2009; Khangulyan et al. 2007) and hadronic interaction of the PW with the dense de-

¹ Department of Astronomy & Astrophysics, Pennsylvania State University, 525 Davey Lab, University Park, PA 16802, USA; ggp1@psu.edu

² George Washington University, 105 Corcoran Hall, Washington, DC 20052, USA

³ Toronto, ON, Canada

⁴ Decretion disks (also known as excretion disks) are viscous gaseous disks around rapidly rotating O or B stars (Be stars) in which stellar matter slowly moves outward and rotates with nearly Keplerian velocity in the equatorial plane (see Rivinius et al. 2013 for a recent review).

cretion disk (Aharonian et al. 2009).

The size of the B1259 binary is too small to resolve it in X-rays, but the high angular resolution of the *Chandra X-ray Observatory* (*CXO*) allows one to look for extended emission from the pulsar wind nebula (PWN) or from matter that could be expelled from the binary. First detection of extended emission associated with B1259 was reported by Pavlov et al. (2011). They observed B1259 with *CXO* on 2009 May 14 (ObsID 1089; 26 ks exposure), when the pulsar just had passed the apastron of 2009 April 5 (see Figure 1), and detected faint, asymmetric extended emission seen up to $\approx 4''$ south-southwest from the binary position. This emission was interpreted as a PWN blown out of the binary by the massive companion’s wind.

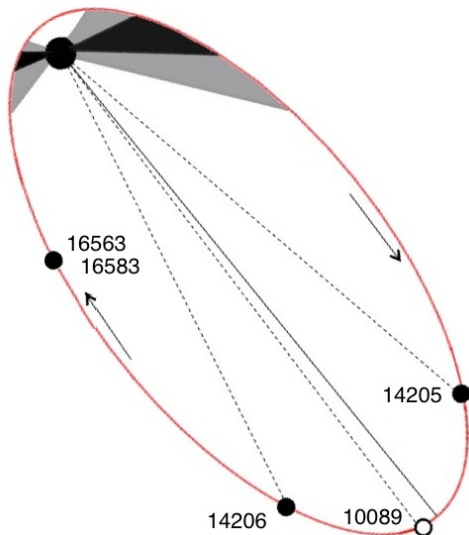


FIG. 1.— Orbital locations of the pulsar at the times of our *Chandra* ACIS observations, marked by their ObsIDs. Our ‘new data’ consists of two exposures (ObsIDs 16563 and 16583) separated by about 10 hours. Gray areas show the parts of the orbit where the pulsar passes through the companion’s equatorial disk.

Kargaltsev et al. (2014; referred to as K+14 hereafter) reported results of two deeper *CXO* observations (ObsIDs 14205 and 14206; 56 ks exposures). These observations were carried out on 2011 December 17 and 2013 May 19, i.e., 370 and 886 days after the periastron of 2010 December 14. They revealed a variable, extended (about $4''$, ~ 1000 times the binary orbit size) structure, which appeared to shift by $1''.8 \pm 0''.5$ between the two observations. K+14 discussed two possible interpretations of the observed variability: (1) an extrabinary termination shock in the PW outflow, with a variable stand-off distance, or (2) a clump ejected from the binary and moving with a projected velocity $v_{\perp} = (0.046 \pm 0.013)c$, at $d = 2.3$ kpc. The analysis of those data favored the scenario in which most of the observed extended emission would come from the PW launched from the binary near the apastron of 2009. To gain a better understanding of

the observed phenomenon and test our interpretations, we proposed a Director Discretionary Time (DDT) *CXO* observation. Here we report the results of the new observation, analyze it jointly with the two previous observations (taken within the same orbital cycle between the periastrons of 2010 and 2014), and suggest a new interpretation of the extended structure.

2. OBSERVATIONS AND DATA REDUCTION

B1259 was observed with the Advanced CCD Imaging Spectrometer (ACIS) on-board *CXO* on 2014 February 8 and 9 (ObsIDs 16563 and 16583, respectively), with a total live time of 57.6 ks. The corresponding orbital location of the pulsar (≈ 1150 days after the periastron of 2010; $\theta = 221^{\circ}$) is shown in Figure 1. The observation setup was similar to our previous observations that have been analyzed in K+14. The target was imaged on the front-illuminated ACIS-I3 chip in timed exposure mode, the data were telemetered in ‘very faint’ format. A $1/8$ subarray was used to reduce the frame time to 0.4 s and mitigate the effect of pile-up. The highest count rate observed from the binary (0.043 counts per frame) corresponds to a negligibly small pile-up fraction of $< 2\%$.

We used the pipeline-produced Level 2 event files for the analysis. No episodes of anomalously high background rates occurred in the observations. To minimize the background contribution, we filtered the events by limiting the photon energies to 0.5 – 8 keV. The detector response for spectral analysis was produced with CIAO (ver. 4.6) tools, following the standard procedure and using the calibration database CALDB 4.5.9. The spectral fitting was done with XSPEC (ver. 12.8.0).

3. DATA ANALYSIS

3.1. Apparent motion of the extended feature

Since the two new observations were carried out less than one day apart, we merged the data for purposes of image analysis. The merged image clearly reveals a ‘blob’ of extended emission with a very faint westward extension. The appearance of the extended feature has changed substantially between the preceding observation ObsID 14206 and the new data (see Figure 2). Unlike the earlier images, in which the feature resembled an arc, the feature’s shape is more round in the new image. It is possible that the fainter part of the feature had simply become too faint to be detected as a result of a decrease in the surface brightness.

The new data allow us to further track the motion of the extended feature reported in K+14. Using the CIAO `celldetect` tool, we measured the positions of the binary and the extended feature together with the corresponding 1σ uncertainties⁵. The $3''.1 \pm 0''.7$ shift of the blob, with respect to the position of the arc-like structure in the ObsID 14206 image, corresponds to a proper motion $\mu = 4''.2 \pm 0''.9 \text{ yr}^{-1}$ and projected velocity $v_{\perp} = (0.15 \pm 0.04)c$, at $d = 2.3$ kpc. The temporal dependence of the radial separation of the extended emission from

⁵ For the elongated arc-like structure in the earlier images, K+14 used a different method (see Figure 3 in K+14), but running `celldetect` on ObsID 14206 gave consistent results. For ObsID 14205 `celldetect` fails to pick out the azimuthally extended structure because it was too close to the bright binary, so we used the peak in the radial count distribution for the blob position and the FWHM of the peak for its uncertainty.

the binary, at a position angle of 215° (north through east), is plotted in Figure 3. The plot does not show any evidence of deceleration, rather it might suggest that the blob is moving with an acceleration $\dot{v}_\perp \sim \Delta v_\perp / \Delta t \sim (0.010 \pm 0.04)c / (390 \text{ d}) = 90 \pm 40 \text{ cm s}^{-2}$. Given the low significance of this result, we assumed a constant velocity and estimated it by fitting the radial separations with a straight line, $r(t) = \mu(t - t_0) + r_0$, where $t_0 = 801$ days is the reference time (all times are counted from the periastron of 2010 December 14). The fit yields $r_0 = 4''.6 \pm 0''.4$, $\mu = 0''.0056 \pm 0''.0009 \text{ d}^{-1} = 2''.0 \pm 0''.3 \text{ yr}^{-1}$. This proper motion corresponds to the projected velocity $v_\perp = (0.07 \pm 0.01)c$ at $d = 2.3 \text{ kpc}$. The launch time, defined as $r(t_{\text{launch}}) = 0$, is $t_{\text{launch}} = -21_{-165}^{+122}$ days. This range of t_{launch} encompasses the periastron and the *Fermi* flare dates.

3.2. Spectral analysis

We extracted the spectra from each of the two new observations and fitted them simultaneously. The extraction regions are shown in Figure 2. We fit the spectra of the compact core (6257 counts in the $0''.9$ radius aperture) and the blob (58 counts in the 3.6 arcsec^2 area) with the absorbed power-law model, using the XSPEC `phabs` model for absorption. We obtained the following fitting parameters for the core: photon index $\Gamma = 1.5 \pm 0.4$, hydrogen column density $N_H = (4.2 \pm 0.3) \times 10^{21} \text{ cm}^{-2}$, and unabsorbed flux $F_{0.5-8 \text{ keV}}^{\text{unabs}} = (1.95 \pm 0.04) \times 10^{-12} \text{ erg cm}^{-2} \text{ s}^{-1}$ (see Table 1 for more details).

Because of the small number of counts in the blob, we used C-statistic⁶ (without binning) and fixed N_H to fit its spectrum. The fitting parameters are provided in Table 1. Figure 4 shows the 90% and 99% confidence contours in the Γ - \mathcal{N} plane (\mathcal{N} is the power-law normalization) for $N_H = 3 \times 10^{21} \text{ cm}^{-2}$. The latter value is smaller than the one we obtained from fitting the core spectrum; we chose it as the average of the N_H values obtained in the fits of the core spectrum in ObsIDs 14205 and 14206 (K+14) in order to exclude additional absorption from within the binary itself. Figure 4 also shows the Γ - \mathcal{N} confidence contours for the extended emission from two previous observations, which we re-fit using the C-statistic for consistency. We see that the photon index for the blob in the new data, $\Gamma = 0.8 \pm 0.4$, does not exceed those found in the previous observations, $\Gamma = 1.2 \pm 0.2$ and 1.3 ± 0.2 for ObsIDs 14205 and 14206, respectively (i.e., the spectral evolution does not show any cooling of the blob's matter). We see from Figure 4 that the flux of extended emission has been steadily decreasing. Fitting it with an exponential decay law yields a characteristic decay time of 540 ± 100 days.

4. DISCUSSION

K+14 have discussed possible scenarios regarding the origin and nature of the observed variable extended emission. One possibility considered by K+14 was the synchrotron emission from the PW that escapes from the binary in the direction away from the high-mass star and shocks in the extrabinary medium, similar to PWNe of young solitary pulsars (Kargaltsev & Pavlov 2008). The

estimated stand-off distance to such a shock is comparable to the observed separations for an ambient pressure $p_{\text{amb}} \sim 10^{-10} \text{ dyn cm}^{-2}$. Because of the large eccentricity of the binary, the pulsar spends most of orbital cycle around apastron, so most of the shocked PW matter concentrates around the extension of the binary's major axis in the apastron direction. The separation between the extrabinary shock and the pulsar could vary due to changes of the ratio of the PW pressure to the ambient pressure. However, this interpretation looks somewhat artificial now because the new data strongly suggest that the separation is steadily increasing, which would require a steadily decreasing ambient pressure (or increasing PW pressure) on a time scale of ~ 800 days. In addition, the required ambient pressure is unrealistically high for a circumbinary medium, which is likely filled with a freely flowing stellar wind of the massive companion, and the extended structure does not have an arc-like appearance anymore, hence losing its resemblance to a termination shock.

Another scenario considered by K+14 assumed that the moving structure is a clump of matter ejected from the binary by the pulsar interaction with the decretion disk. The new data seem to support this scenario because the average projected velocity implies that the structure could indeed be launched near periastron. However, as K+14 pointed out, the fast, steady motion over such a large period of time poses a number of problems. If the ejected clump consists solely of synchrotron-emitting relativistic electrons or positrons, possibly confined by the magnetic field, it should decelerate very quickly by the drag force (assuming it moves through a much slower expanding medium, such as a bubble created by the companion's wind). On the other hand, if the clump consists solely of electron-ion plasma (e.g., a fraction of the decretion disk heated and expelled from the binary by the interaction with the PW)⁷, then its mass would be $m_{\text{cl}} \sim 10^{29} \text{ g}$, much larger than the plausible mass of the disk, $m_{\text{disk}} \sim 10^{24} - 10^{26} \text{ g}$ (Chernyakova et al. 2014, and references therein), or the mass $\dot{M}P_{\text{orb}} = 6.7 \times 10^{25} (\dot{M}/10^{-8} M_\odot/\text{yr}) \text{ g}$ lost by the high-mass companion during one orbital cycle. In addition, its kinetic energy, $E_{\text{cl}} \sim 10^{47} \text{ erg}$, would exceed the energy that could be supplied by any conceivable source.

A mixed scenario, in which the emission is produced by relativistic electrons supplied by the PW but the clump's mass is determined by protons/ions from the stellar outflow, may be more plausible. However, even in this scenario, the clump's mass should be a substantial fraction of m_{disk} to overcome the drag force, even at extremely low ambient densities (K+14). Moreover, it remains unclear what is the source of the corresponding clump's kinetic energy, $E_{\text{cl}} \sim 5 \times 10^{43} (m_{\text{cl}}/10^{25} \text{ g})(v/0.1c)^2 \text{ erg}$, let alone the acceleration mechanism. If the clump's energy is provided by the loss of a small fraction of the pulsar's spin energy, $E_{\text{sp}} = 8.6 \times 10^{48} \text{ erg}$ (for the moment of inertia $I = 10^{45} \text{ g cm}^2$), during the disk passage, the decrease of the spin energy, $\Delta E_{\text{sp}} \sim E_{\text{cl}}$, would lead to a perceptible increase of the spin period,

⁷ In this case, the clump emission would be thermal bremsstrahlung. As shown by K+14, the spectra of the extended feature can be fitted by a thermal bremsstrahlung model with $kT \gtrsim 10 \text{ keV}$, $n_e \sim n_p \sim 10^2 \text{ cm}^{-3}$.

⁶ <https://heasarc.gsfc.nasa.gov/xanadu/xspec/manual/XSappendixStatistics.html>

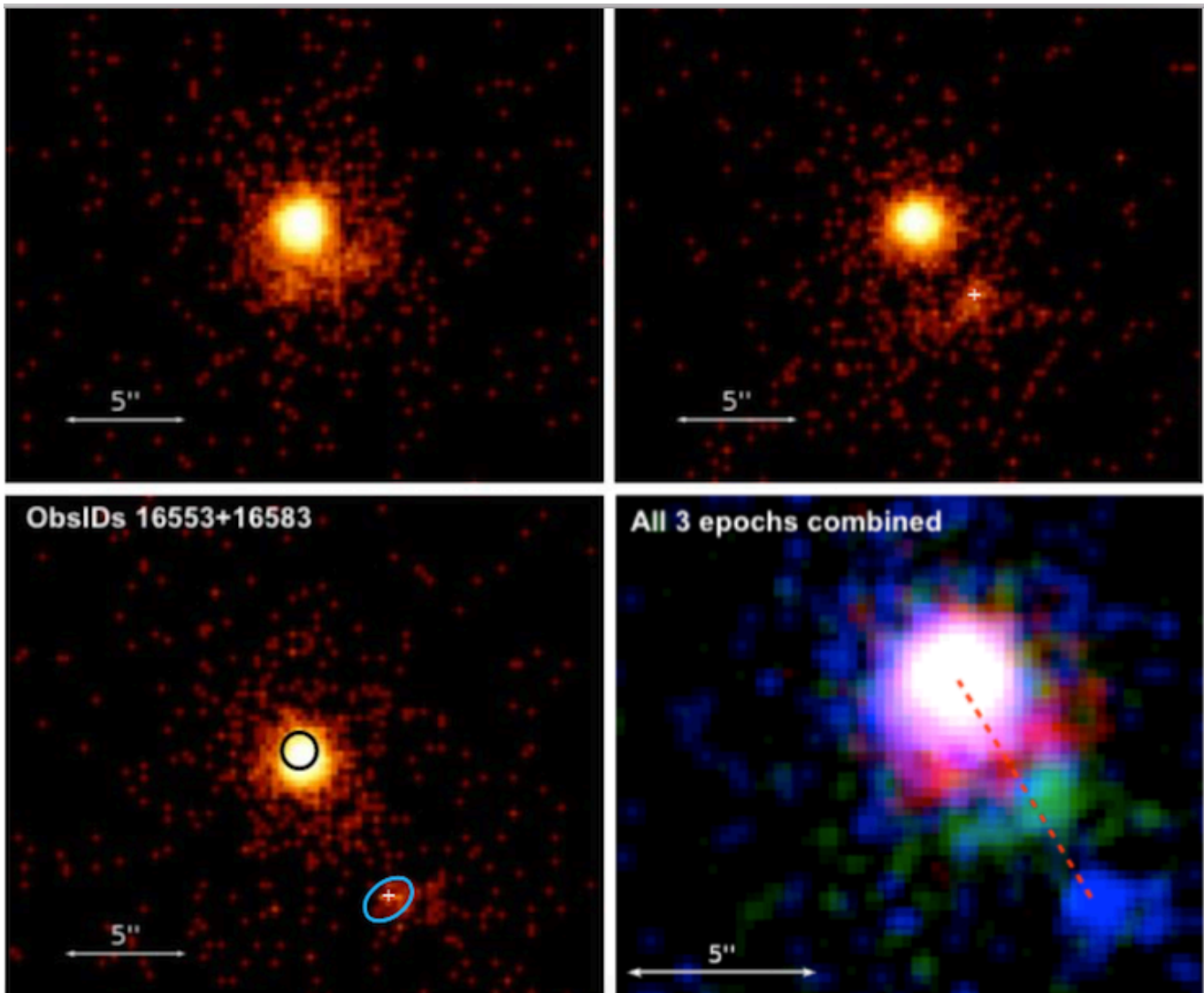


FIG. 2.— ACIS images from our previous two observations, ObsIDs 14205 (top left) and 14206 (top right), and the new data (bottom left). The blob of extended emission is clearly traveling away from the binary. The bottom right panel shows the false color image (different colors correspond to different observation epochs) demonstrating the motion and changes in morphology. The dashed line connects the binary and the centroid of the feature in the new data image. The angular separation between the extended feature and the binary as a function of time is shown in Figure 3. The spectral extraction regions (core and extended emission are shown in black and cyan, respectively) on new data image. North is up, east is to the left. The radius of the black circle is $0''.9$; the background extraction region (not shown) is an annulus with radii $8''.55 \leq r \leq 19''.18$. The white crosses mark the positions of the extended emission as obtained with the CIAO `celldetect` tool. The apparent asymmetry of the bright core seen in the merged image of ObsIDs 16563+16583 can, at least partly, be attributed to the known Chandra mirror asymmetry.

$\Delta P \sim (P^3/4\pi^2 I)E_{\text{cl}} \sim 6 \times 10^{-8} (m_{\text{cl}}/10^{25} \text{ g}) \text{ s}$. However, no such period jumps were noticed in the most detailed timing analysis available (Shannon et al. 2014). These authors mention systematic variations in timing residuals close to the 6 periastron passages covered by their analysis, but they attribute those to uncorrected variations in dispersion measure or scattering of the pulsar radiation through the disk. Thus, it seems that the spin-down due to the pulsar-disk interaction does not look as a plausible source of the clump energy. In principle, one might assume that a small fraction of pulsar’s kinetic energy, $E_{\text{kin}} \sim 10^{48}$ erg (near periastron), is somehow converted into the clump’s energy in the course of pulsar-disk interaction, but a decrease of E_{kin} should result in a decrease of binary period P_b , which is not consistent

with the results of timing analysis⁸. Thus, we conclude that even the mixed clump scenario looks problematic because ejection of a large mass is required to overcome the drag force, and it remains unclear what is the energy source and how such a mass could be accelerated to a velocity $\sim 0.1c$ during the short time of the pulsar-disk interaction.

The drag deceleration and energy deficit problems can be alleviated if, instead of the companion’s wind bubble, *the clump is moving in the unshocked PW* whose velocity, close to the speed of light, significantly exceeds the

⁸ On the contrary, Shannon et al. (2014) found a hint of *increase* of the binary period, with a derivative $\dot{P}_b = (1.4 \pm 0.7) \times 10^{-8} \text{ s s}^{-1}$, corresponding to $\Delta P_b \approx 1.5 \text{ s}$ per binary cycle, which they attribute to mass loss due to the polar wind of LS 2883.

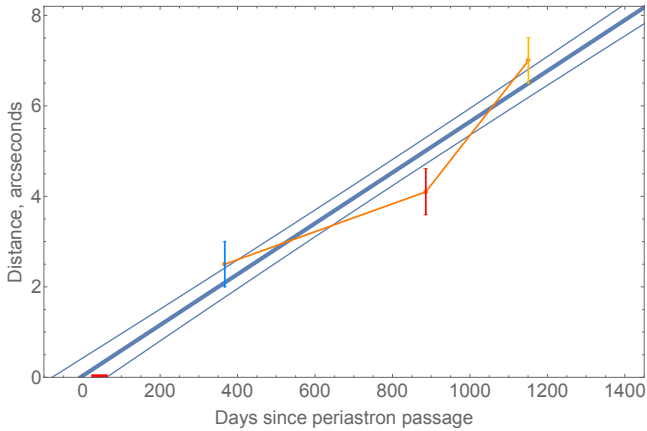


FIG. 3.— Separation of the extended feature from the unresolved point source (in arcseconds) as a function of time since the periastron passage on 2010 December 14. The line of best fit and 1σ upper and lower bounds are also shown. The small red line at the bottom shows the time period, 2011 January 14 – March 4, in which the GeV flare occurred (Abdo et al. 2011).

clump’s velocity. This scenario becomes more plausible at larger values of the parameter $\eta = \dot{E}/(\dot{M}v_w c) = 4.4 \dot{M}_{-9}^{-1} v_{w,8}^{-1}$, where \dot{M}_{-9} is the mass-loss rate in the O-star polar wind⁹ in units of $10^{-9} M_{\odot} \text{ yr}^{-1}$, and $v_{w,8}$ is the wind’s velocity in units of 1000 km s^{-1} . At $\eta > 1$, the companion’s wind is confined by the PW into a cone with half-opening angle $\alpha \approx 30^\circ (4 - \eta^{-2/5}) \eta^{-1/3}$ (Eichler & Usov 1993), while the unshocked PW fills the rest of circumbinary volume¹⁰. Since the pressure in the freely flowing (unshocked) polar wind of the high-mass companion is proportional to r^{-2} , similar to the PW ram pressure, $p_{\text{pw}} = \dot{E}/(4\pi cr^2) = 2.2 \times 10^{-10} r_{17}^{-2} \text{ dyn cm}^{-2}$ (where $r_{17} = r/10^{17} \text{ cm}$), the PW cannot shock until it reaches the termination shock of the stellar wind at $r = r_{\text{ts}}$, where the wind bubble pressure jumps up by a few orders of magnitude (see Figure 1 in Dwarkadas 2005). This means that the PW shocks at large distances from the binary (e.g., at $\sim 3'$ for $r_{\text{ts}} \sim 2 \text{ pc}$), where the surface brightness of the shocked PW emission (PWN) may be too low to be detected. In this scenario, the observed extended X-ray emission can be due to synchrotron radiation of the PW shocked by the collision with the clump of ejected material. The X-ray luminosity can be estimated as $L_{X,\text{cl}} = \eta_X \dot{E} (r_{\text{cl}}/2r)^2$, where r is the distance from the pulsar, r_{cl} is the effective radius of the clump, and η_X is the X-ray efficiency.

⁹ The reference value of mass-loss rate, $\dot{M} = 10^{-9} M_{\odot} \text{ yr}^{-1}$, is lower than usually adopted for LS 2883, but such a low \dot{M} is consistent with observations of OV stars with luminosities $L_* < 10^{5.3} L_{\odot}$, which show mass losses lower than theoretically predicted or expected from extrapolations from more luminous O stars (the so-called “weak wind problem”; see Section 5 in the review by Puls et al. 2008.)

¹⁰ A large value of η is needed in our scenario because in the opposite case the unshocked PW would occupy only a narrow channel confined by the stellar wind and rotating around the massive star together with the pulsar. Even if a clump of stellar matter gets into that channel, it will go out from the channel in a fraction of the binary period and will be decelerated by the stellar wind. We note that larger η also imply the intra-binary shock is closer to the massive star, which helps to explain the high-energy emission by the Compton up-scattering of stellar photons (Sierpowska-Bartosik & Bednarek 2008).

For instance, $L_{X,\text{cl}} \sim 0.01 \eta_X \dot{E} \sim 8 \times 10^{33} \eta_X \text{ erg s}^{-1}$ for $r_{\text{cl}}/r \sim 0.2$ for the latest observation. This estimate is consistent with the observed X-ray luminosity, $L_{X,\text{cl}} = (1.3 \pm 0.3) \times 10^{31} d_{2,3}^2 \text{ erg s}^{-1}$, at a reasonable value for X-ray efficiency, $\eta_X \sim 1.5 \times 10^{-3}$. This interpretation of the X-ray emission is also consistent with the lack of spectral softening (Section 3.2) because cooling of relativistic electrons is compensated by the energy supplied by the PW.

The interaction of the unshocked PW with the ejected fragment is not only responsible for its X-ray emission, but it can also *accelerate* the fragment. A very crude estimate of acceleration is $\dot{v} \sim p_{\text{pw}} A m_{\text{cl}}^{-1} \sim 440 r_{17}^{-2} \xi_A (m_{\text{cl}}/10^{21} \text{ g})^{-1} \text{ cm s}^{-2}$, where p_{pw} is the PW ram pressure, $A \sim 2 \times 10^{33} \xi_A \text{ cm}^2$ is the clump’s cross section, and $\xi_A < 1$ is the filling factor¹¹. Interestingly, this estimate is consistent with the apparent acceleration estimated (with low significance) in Section 3.1 at $m_{\text{cl}} \sim 10^{21} \xi_A \text{ g}$ (for $r = 2 \times 10^{17} \text{ cm}$, i.e., $\sim 7''$ from the pulsar). Ejection of such a small mass should not make a measurable effect on pulsar timing. Moreover, the possibility of gradual acceleration of the ejected clump alleviates the problem of a huge acceleration of the clump in the course of its ejection caused by pulsar-disk interaction. For instance, for $m_{\text{cl}} \sim 10^{21} \text{ g}$, the clump’s kinetic energy, $E_{\text{cl}} \sim 4.5 \times 10^{39} (v/0.1c)^2 \text{ erg}$, is a tiny fraction, $\sim 5 \times 10^{-5}$, of the pulsar’s spin-down energy loss during, e.g., the time elapsed from the 2010 periastron. We should note that if the acceleration during our observations was indeed so large, then the conclusion that the clump was launched around the 2010 periastron, derived under the assumption of constant speed, becomes questionable (unless the acceleration was much lower when the clump was closer to the binary, e.g., due to a larger accelerated mass). The matter could be ejected by the pulsar-disk interaction close to an earlier periastron, but it is hardly possible to estimate the launch time without detailed modeling of the PW-clump interaction, accounting for varying acceleration.

A qualitative scenario for cloud formation and acceleration might look as follows. Before entering the disk, the pulsar moves in the fast, radially directed companion’s polar wind, the apex of the intrabinary bow shock is on the line connecting the pulsar and the companion, and the shock position and shape are determined by the parameter η (Dubus 2013). When the pulsar enters the disk, the structures of both the disk and the intrabinary shock change dramatically. Since the matter in the disk moves in almost circular orbits around the companion with nearly Keplerian velocity (Rivinius et al. 2013), which is comparable to the orbital velocity of the pulsar, the relative velocity of the pulsar and the disk matter, $\mathbf{v}_{\text{rel}} = \mathbf{v}_{\text{disk}} - \mathbf{v}_{\text{psr}}$, is not directed radially, and the shock apex is not on the pulsar-companion line (see an illustration in Khangulyan et al. 2012). The (minimum) distance of the shock from the pulsar can be estimated as $r_s \sim \dot{E}^{1/2} [4\pi c \rho_{\text{disk}}(R)]^{-1/2} |\mathbf{v}_{\text{rel}}(R)|^{-1}$, where $\rho_{\text{disk}}(R) \sim \rho_0 (R_*/R)^3$ is the density in the mid-

¹¹ The ‘clump’ can consist of a few smaller fragments, which we cannot resolve in the image. These fragments could be launched from the binary in slightly different directions, which could explain the large size of the observed extended feature.

TABLE 1
SPECTRAL FIT PARAMETERS FOR THE CORE AND EXTENDED EMISSION IN THREE CXO ACIS-I OBSERVATIONS

ObsID	MJD	θ^a deg	Δt^b days	Exp. ^c ks	Cts ^d	F_{obs}^e 10^{-14} cgs	F_{corr}^f 10^{-14} cgs	N_H 10^{21} cm^{-2}	Γ	\mathcal{N}^g 10^{-4}	\mathcal{A}^h (arcsec^2)	χ^2/dof
10089	54965	182	667	25.6	1825	139(5)	158(6)	1.5(7)	1.51(10)	2.3(3)	2.5	20.9/30
					61	2.8(1)	3.1(1)	1.5*	1.3(5)	0.039(16)	22.1	3.1/9
14205	55912	169	370	56.3	6551	249(4)	296(5)	2.9(3)	1.39(5)	3.8(2)	2.5	76.6/87
					343	8.5(5)	9.2(7)	2.9*	1.2(1)	0.10(1)	22.1	36.24% ^k
14206	56431	192	886	56.3	4162	137(5)	176(7)	3.1(3)	1.68(6)	3.07(2)	2.5	146/169
					144	3.6(4)	3.9(6)	3.1*	1.3(2)	0.052(14)	12.8	62.96% ^k
<i>New</i> ⁱ	56696	221	1151	57.6	6257	149(5)	195(4)	4.2(3)	1.5(4)	3.0(1)	2.5	242.5/204
					58	1.9(4)	2.0(4)	3.0* ^j	0.8(4)	0.013(7)	3.6	54.12% ^k

NOTE. — For each ObsID the upper and the lower rows correspond to the partially resolved core and the extended emission, respectively. The 1σ uncertainties are shown in parentheses (see also Figure 4). The XSPEC extinction model `phabs` was used throughout. Fluxes and counts are in the 0.5–8 keV range, corrected for finite aperture size for the core emission. An asterisk indicates that the extinction column was fixed to the value of the corresponding point source fit.

^a True anomaly counted from periastron.

^b Days since latest preceded periastron.

^c Exposure corrected for deadtime.

^d Total (gross) counts.

^e Observed flux.

^f Extinction corrected flux.

^g Normalization in photons $\text{s}^{-1} \text{cm}^{-2} \text{keV}^{-1}$ at 1 keV.

^h Area of the extraction region.

ⁱ ObsIds 16563 and 16583 fit simultaneously.

^j Fit was done, for extended emission, using the fixed N_H value obtained from fitting the core around apastron passage to exclude any absorption from within the binary.

^k C-statistics were used for fitting the extended emission spectra across all observations for consistency. This percentage is the Null Hypothesis probability $1 - \mathcal{P}$, where \mathcal{P} is the probability given by the XSPEC `goodness` command with 10,000 runs.

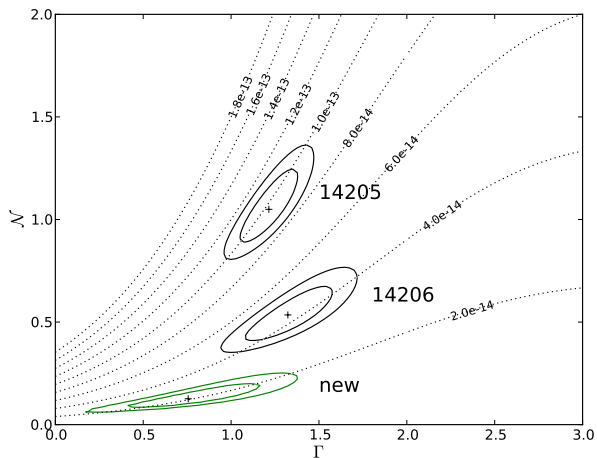


FIG. 4.— Confidence contours (90%, and 99%) in the Γ - \mathcal{N} plane for the ACIS spectra of the extended nebula (see Figure 3 and K+14 for region definitions) computed for the absorbed PL model. The PL normalization \mathcal{N} is in units of 10^{-5} photons $\text{cm}^{-2} \text{s}^{-1} \text{keV}^{-1}$ at 1 keV. The dashed lines are lines of constant unabsorbed flux in the 0.5–8 keV band (labeled in $\text{erg cm}^{-2} \text{s}^{-1}$). The contours for observations 14205, 14206 and the new data were fit with N_H fixed at the values of $N_H = 2.9, 3.1, 3.0 \times 10^{21} \text{ cm}^{-2}$, respectively.

plane of the disk in the pulsar vicinity (at the distance R from the companion), $R_* \sim 10R_\odot$ is the companion’s radius. Using the same disk model as Chernyakova et al. (2014), we obtain the shock radius $r_s \sim 1.5 \times 10^{13} (\rho_{\text{disk}}/10^{-16} \text{ g cm}^{-3})^{-1/2} (v_{\text{rel}}/100 \text{ km s}^{-1})^{-1} \text{ cm}$, for the first crossing of the disk ($R \sim 40R_* \sim 2 \text{ AU}$). Since r_s exceeds (or is comparable to) the vertical size of the disk, $H(R = 40R_*) \sim 5 \times 10^{12} \text{ cm}$, the disk should be significantly disrupted by the first pulsar passage, which

is consistent with numerical simulations (Okazaki et al. 2011; Takata et al. 2012). In the second disk passage further fragmentation of the disk can occur. The collision of the PW with disk matter fragments would result in shocks and γ -ray flares from the shocked PW, as well as entrainment of the clumps in the PW flow, which would blow them out of the binary and eventually accelerate up to the observed velocity $\sim 0.1c$. The details of the mass loading and ejection processes are likely very complex and should be investigated with numerical simulations.

A possible mechanism of matter ejection from the binary could be connected with episodic accretion of the disk matter onto the neutron star magnetosphere¹². If there were no PW and associated shock, the neutron star moving in the decretion disk could gravitationally capture the matter within the cylinder of radius $R_{\text{grav}} = 2GM_{\text{psr}}v_{\text{rel}}^{-2} = 3.7 \times 10^{12} (v_{\text{rel}}/100 \text{ km s}^{-1})^{-2} \text{ cm}$ (for $M_{\text{psr}} = 1.4M_\odot$), with the maximum possible capture rate $\dot{m}_{\text{max}} = \pi R_{\text{grav}}^2 \rho_{\text{disk}} v_{\text{rel}} = 4.4 \times 10^{16} (\rho_{\text{disk}}/10^{-16} \text{ g cm}^{-3}) (v_{\text{rel}}/100 \text{ km s}^{-1})^{-3} \text{ g s}^{-1}$. However, if the radius r_s of the PW shock exceeds R_{grav} (as for the parameters assumed above for the shock radius estimate), the matter is deflected by the shock out of the capture cylinder. Nevertheless, the capture becomes possible if $R_{\text{grav}} > r_s$, i.e., if $\rho_{\text{disk}} > 1.6 \times 10^{-15} (v_{\text{rel}}/100 \text{ km s}^{-1})^2 \text{ g cm}^{-3}$. If the disk density is indeed so high in the vicinity of the crossing pulsar (which is not ruled out — see Takata et al. 2012), then the ram pressure of the gravitationally attracted matter ($\rho v_{\text{ff}}^2 \propto r^{-5/2}$) overcomes the ram pressure of the PW ($p_{\text{pw}} \propto r^{-2}$), and the disk matter

¹² Accretion onto the neutron star surface would be inconsistent with the relatively low X-ray luminosity of B1259 even around periastron.

streams toward the pulsar with a nearly free-fall velocity, $v_{\text{ff}} = (2GM_{\text{psr}}/r)^{1/2}$, until it reaches the pulsar magnetosphere at $r \sim R_{\text{lc}} = cP/(2\pi) = 2.3 \times 10^8$ cm. At radii smaller than the light cylinder radius R_{lc} the accreting matter is stopped by the magnetic field pressure ($B^2/8\pi \propto r^{-6}$) in the pulsar magnetosphere, at the Alfvén radius $R_A \sim (8GM_{\text{psr}})^{-1/7} \mu^{4/7} \dot{m}^{-2/7} \sim 1.4 \times 10^8 \dot{m}_{17}^{-2/7}$ cm, where $\mu = B_{\text{NS}} R_{\text{NS}}^3 \sim 3.3 \times 10^{29}$ G cm³ is the pulsar’s magnetic moment, and $\dot{m}_{17} = \dot{m}/(10^{17} \text{ g s}^{-1})$. As long as R_A exceeds the corotation radius $R_{\text{cor}} = (GMP^2/4\pi)^{1/3} = 2.2 \times 10^7$ cm (i.e., at any reasonable accretion rate $\dot{m} < 6 \times 10^{19} \text{ g s}^{-1}$), accretion occurs in the ‘propeller regime’ (Illarionov & Sunyaev 1975), i.e., the accreting matter does not reach the neutron star surface. Most of this matter is expelled in a disk-shaped outflow in the equatorial plane by the centrifugal forces (see Romanova et al. 2003 for MHD simulations) while up to $\sim 10\%$ can leave the system in a high-velocity jet along the neutron star spin axis¹³ (Lovell et al. 2014, and references therein), with a velocity up to $(GM/R_A)^{1/2} \sim 0.04\dot{m}_{17} c$. An upper limit on the total mass ejected in a jet during the disk passage can be as large as $\sim 0.1\dot{m}t_{\text{disk}} \sim 10^{22}\dot{m}_{17}(t_{\text{disk}}/15 \text{ d}) \text{ g}$. If the ejected matter gets into the region of unshocked PW, it can be further accelerated to the observed velocity of $\sim 0.1c$. Thus, accretion of decretion disk matter in the propeller regime could, in principle, be responsible for ejection of the observed clump, but it would require a rather high accretion rate (i.e., a very large disk density).

Overall, the interpretation of the moving extended X-ray feature as a fragment of the decretion disk ejected from the binary by the pulsar-disk interaction and moving in the unshocked PW looks quite plausible. However, we should mention a possible contradiction between such an interpretation and the detections of extended radio emission around the pulsar 29 days after the 2010 periastron (Chernyakova et al. 2014) and 21 days after the 2007 periastron (Moldón et al. 2011). That emission, with a total size of ~ 50 mas (115 AU at $d = 2.3$ kpc) and a larger extension toward northwest, was interpreted as a cometary tail extending behind the pulsar in the northwest direction, quite different from the southwest direction of the X-ray feature motion. To reconcile the

different directions, we have to assume that the radio and X-ray features are intrinsically different (e.g., comprised of different matter) or that the ejected fragment could change the direction of its motion because of the varying direction of the accelerating force close to the binary.

5. CONCLUSIONS

Our new *CXO* observation of the extended object in the vicinity of the B1259 binary has shown that the object keeps moving away from the binary. The comparison with two previous observations shows that its luminosity has been steadily decreasing, and its average projected velocity was $v_{\perp} \approx 0.07c$ during 780 days covered by the observations. If that velocity has remained constant in the course of motion, the object was ejected from the binary near the 2010 periastron, perhaps by the collision of the pulsar with the decretion disk of the high-mass companion. If this clump of matter were moving in a slowly expanding circumbinary medium, its mass and kinetic energy would be uncomfortably large to overcome the drag deceleration. Therefore, we suggest the clump (likely a fragment of the decretion disk) is moving in the unshocked relativistic PW. Its X-ray emission can be interpreted as synchrotron radiation of the PW shocked by an interaction with the fragment. The ram pressure of the PW can be responsible for clump acceleration, a hint of which is seen in our observations. No such phenomena have been observed so far. Further monitoring with *CXO* is needed to confirm or refute this interpretation.

Support for this work was provided by the National Aeronautics and Space Administration through *Chandra* Awards DD3-14070 and GO2-13085 issued by the *Chandra* X-ray Observatory Center, which is operated by the Smithsonian Astrophysical Observatory for and on behalf of the National Aeronautics Space Administration under contract NAS8-03060. We are very grateful to Harvey Tananbaum for allocating the DDT time to continue monitoring this system. We also thank Dmitry Khangulyan for useful discussions and the anonymous referee for careful reading of the paper and useful comments.

Facility: CXO

REFERENCES

- Abdo, A. A., Ackermann, M., Ajello, M., et al. 2011, *ApJ*, 736, L11
- Aharonian, F., Akhperjanian, A. G., Aye, K.-M., et al. 2005, *A&A*, 442, 1
- Aharonian, F., Akhperjanian, A. G., Anton, G., et al. 2009, *A&A*, 507, 389
- Ball, I., Melatos, A., Johnston, S., & Skjæ Raasen, O. 1999, *ApJL*, 514, L39
- Chernyakova, M., Neronov, A., Lutovinov, A., Rodriguez, J., & Johnston, S. 2006, *MNRAS*, 367, 1201
- Chernyakova, M., Neronov, A., Aharonian, F., Uchiyama, Y., & Takahashi, T. 2009, *MNRAS*, 397, 2123
- Chernyakova, M., Abdo, A. A., Neronov, A., et al. 2014, *MNRAS*, 439, 432
- Dubus, G. 2013, *A&A Rev.*, 21, 64
- Dwarkadas, V. V. 2005, *ApJ*, 630, 892
- Eichler, D., & Usov, V. 1993, *ApJ*, 402, 271
- Illarionov, A. F., & Sunyaev, R. A. 1975, *A&A*, 39, 185
- Johnston, S., Manchester, R. N., Lyne, A. G., Bailes, M., Kaspi, V. M., Qiao, G., & D’Amico, N. 1992, *ApJ*, 387, L37
- Johnston, S., Ball, I., Wang, N., & Manchester, R. N. 2005, *MNRAS*, 358, 1069
- Kargaltsev, O., & Pavlov, G. G. 2008, in *American Institute of Physics Conference Proceedings*, Vol. 983, 40 Years of Pulsars: Millisecond Pulsars, Magnetars and More, ed. C. Bassa, Z. Wang, A. Cumming, & V. M. Kaspi, 171
- Kargaltsev, O., Pavlov, G. G., Durant, M., Volkov, I., & Hare, J. 2014, *ApJ*, 784, 124 (K+14)
- Khangulyan, D., Hnatic, S., Aharonian, F., & Bogovalov, S. 2007, *MNRAS*, 380, 320
- Khangulyan, D., Aharonian, F. A., Bogovalov, S. V., Ribó, M. 2012, *ApJ*, 752, L17
- Lovell, R. V., Romanova, M. M., Lii, P., & Dyda, S. 2014, *Computational Astrophysics and Cosmology*, 1, 3

¹³ In the numerical simulations of matter flows in the propeller regime (e.g., Romanova et al. 2009) only the case of aligned magnetic and spin axes was considered. We presume that the jet formation can also occur if the axes are misaligned, when the jet should be directed along the the spin axis by the symmetry requirements.

- Malyshev, D., Neronov, A., & Chernyakova, M. 2014, *The Astronomer's Telegram*, 6204, 1
- Melatos, A., Johnston, S., & Melrose, D. B. 1995, *MNRAS*, 275, 381
- Moldón, J., Johnston, S., Ribó, M., Paredes, J. M., & Deller, A. T. 2011, *ApJ*, 732, L10
- Neguera, I., Ribó, M., Herrero, A., Lorenzo, J., Khangulyan, D., & Aharonian, F. A. 2011, *ApJ*, 732, L11
- Okazaki, A. T., Nagataki, S., Naito, T., et al. 2011, *PASJ*, 63, 893
- Pavlov, G. G., Chang, C., & Kargaltsev, O. 2011, *ApJ*, 730, 2
- Puls, J., Vink, J. S., Najarro, F. 2008, *A&A Rev.*, 16, 209
- Rivinius, T., Carciofi, A. C., & Martayan, C. 2013, *A&A Rev.*, 21, 69
- Romanova, M. M., Toropina, O. D., Toropin, Yu. M., Lovelace, R. V. E. 2003, *ApJ*, 588, 400
- Romanova, M. M., Ustyugova, G. V., Koldoba, A. V., & Lovelace, R. V. E. 2009, *MNRAS*, 399, 1802
- Shannon, R. M., Johnston, S., & Manchester, R. N. 2014, *MNRAS*, 437, 3255
- Sierpowska-Bartosik, A., & Bednarek, W. 2008, *MNRAS*, 385, 2279
- Takata, J., Okazaki, A. T., Nagataki, S., et al. 2012, *ApJ*, 750, 70
- Tam, P. H. T., Huang, R. H. H., Takata, J., et al. 2011, *ApJ*, 736, LL10
- Tam, P. H. T., Li, K. L., Takata, J., et al. 2015, *ApJL*, 798, L26
- Tavani, M., & Arons, J. 1997, *ApJ*, 477, 439